ACS APPLIED MATERIALS & INTERFACES

Research Article

www.acsami.org

Immobilization Studies of an Engineered Arginine–Tryptophan-Rich Peptide on a Silicone Surface with Antimicrobial and Antibiofilm Activity

Kaiyang Lim,[†] Ray Rong Yuan Chua,[‡] Rathi Saravanan,[§] Anindya Basu,[†] Biswajit Mishra,[†] Paul Anantharajah Tambyah,[‡] Bow Ho,[‡] and Susanna Su Jan Leong*[,†]

[†]School of Chemical and Biomedical Engineering, Nanyang Technological University, 62 Nanyang Drive, 637459 Singapore

[‡]Yong Loo Lin School of Medicine, National University of Singapore, 1E Kent Ridge Road, 119228 Singapore

[§]School of Materials Science and Engineering, Nanyang Technological University, 50 Nanyang Drive, 637553 Singapore

ABSTRACT: With the rapid rise of antibiotic-resistant-device-associated infections, there has been increasing demand for an antimicrobial biomedical surface. Synthetic antimicrobial peptides that have excellent bactericidal potency and negligible cytotoxicity are promising targets for immobilization on these target surfaces. An engineered arginine–tryptophan-rich peptide (CWR11) was developed, which displayed potent antimicrobial activity against a broad spectrum of microbes via membrane disruption, and possessed excellent salt resistance properties. A tethering platform was subsequently developed to tether CWR11 onto a model polymethylsiloxane (PDMS) surface using a simple and robust strategy. Surface characterization assays such as attenuated total reflectance–Fourier transform infrared spectroscopy (ATR-FTIR), X-ray photoelectron spectroscopy (XPS), and energy-dispersive X-ray spectroscopy (EDX) confirmed the successful grafting of CWR11 onto the chemically treated PDMS surface. The immobilized peptide concentration was 0.8 ± 0.2 $\mu g/cm^2$ as quantitated by sulfosuccinimidyl-4-*o*-(4,4-dimethoxytrityl) butyrate (sulfo-SDTB) assay. Antimicrobial assay and cytotoxic investigation confirmed that the peptide-immobilized surface has good bactericidal and antibiofilm properties, and is also noncytotoxic to mammalian cells. Tryptophan–arginine-rich antimicrobial peptides have the potential for antimicrobial protection of biomedical surfaces and may have important clinical applications in patients.

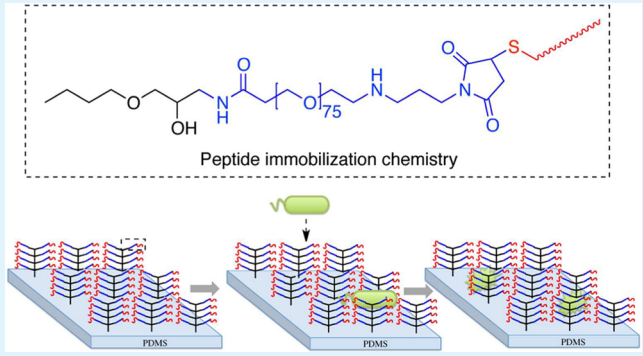

KEYWORDS: *antimicrobial peptide, polymethylsiloxane, antimicrobial surface, peptide immobilization, noncytotoxic, antibiofilm*

1. INTRODUCTION

Natural antimicrobial peptides (AMPs) are an important line of defense in an organism's immune response to microbial infection. These peptides possess broad-spectrum bactericidal characteristics and display excellent antibacteria, antifungal,[1,2] and even antiviral[3] traits. In addition to these antimicrobial properties, AMPs could positively modulate immunity[4] and are less likely to induce bacterial resistance.[5] Against the backdrop of rising antibiotics resistance among microbes, AMPs pose as a good alternative to antibiotics. The transmission of antibiotic resistant pathogens especially in hospitals or long-term care facilities in patients with in-dwelling medical devices is increasing globally and has a significant impact on patient outcomes, as well as placing a significant economic burden on healthcare systems. We believe that functionalizing medical devices such as catheters and stents, with AMPs can help to address this problem. However, to serve as effective coating agents, the AMPs must meet several prerequisites, which include the retention of broad-spectrum antimicrobial activity, biocompatibility, and salt-resistant properties in the tethered state. Many naturally occurring peptides, however, lack the ability to retain all these properties simultaneously. In particular, there are indeed very few AMPs that exhibit broad spectrum antimicrobial activity and salt resistance at the same time. Therefore, there is a need to engineer peptides that possess the desired properties, which forms one of the objectives of this study. Short tryptophan- and arginine-rich peptides are hypothesized to improve antimicrobial activity and overcome salt sensitivity problems. A high arginine content helps a peptide to withstand salt-induced charge shielding effects, and will improve the electrostatic interaction between the peptide and anionic bacterial membrane.[6,7] Tryptophans are well-established to have a strong preference for interfacial regions of the lipid bilayer,[8−10] and aids the attachment and insertion of tryptophan-rich peptide to the lipid bilayer. To combine the salt-tolerant property of arginine and the membrane-destabilizing property of tryptophan in a single arginine- and tryptophan-rich peptide, we engineered a

Received: May 7, 2013
Accepted: June 12, 2013
Published: June 12, 2013

   dx.doi.org/10.1021/am401629p | *ACS Appl. Mater. Interfaces* 2013, 5, 6412−6422

tryptophan−arginine-rich synthetic peptide (CWR11) that showed excellent antimicrobial and salt-tolerant properties. An immobilization platform to immobilize CWR11 on a polydimethylsiloxane (PDMS) surface was developed and the peptide-tethered surface demonstrated broad-spectrum antimicrobial activities, antibiofilm abilities, and excellent biocompatible properties. The outcome of this study indicates the feasibility of tethering short AMPs on silicone-based surfaces for effective antimicrobial functionalization to curb biofilm formation and disease development.

2. MATERIALS AND METHODS

2.1. Materials. Wild-type Jelleine-I and the engineered variant peptide (CWR11), having the amino acid sequence CWFWKWWRRRRR-NH_2, were chemically synthesized by GL Biochem (Shanghai, China) at a purity of >90%. Chemicals were procured from Sigma−Aldrich, unless otherwise specified. Bacterial strains used in this study were *Escherichia coli* (ATCC 8739), *Staphylococcus aureus* (ATCC 6538), and *Pseudomonas aeruginosa* (ATCC 9027; PAO1, green fluorescence protein (GFP)-expressing strain).

2.2. Peptide Concentration Determination. Peptide was dissolved in distilled water and the concentration of the peptide was quantified by absorbance using the Beer−Lambert law. Molar absorption coefficient (ε) of the peptide was determined based on an empirical formula developed by Pace et al.[11]

$$\varepsilon\ (280\ \text{nm}) = 5500(\#\text{Trp}) + 1490(\#\text{Tyr}) + 125(\#\text{Cys}) \quad (1)$$

Absorbance measurements of the peptide solutions were performed using a UV/vis spectrophotometer (Boeco S-22, Germany).

2.3. Minimum Inhibitory Concentration (MIC) Assay. Minimum inhibitory concentrations of CWR11 were performed against *Escherichia coli* (*E. coli*), *Staphylococcus aureus* (*S. aureus*), and *Pseudomonas aeruginosa* (*P. aeruginosa*) by using a standard broth microdilution assay.[12] Briefly, wells of a 96-well microplate were filled with 50.0 μL CWR11 peptide at different concentrations (1.6−50.0 μg/mL). 50.0 μL of 10^6 CFU/mL bacterial suspensions were then added to the wells to obtain a final bacterial concentration of 5×10^5 CFU/mL. The microplate was incubated at 37.0 °C for 16 h. 5.0 μL of the cell suspension from each well was plated on a Mueller Hinton (MH) agar plate. The minimum inhibitory concentration (MIC) was determined to be the peptide concentration at which no colony could be observed on the agar plate.

2.4. Circular Dichroism (CD) Spectroscopy. Circular dichroism (CD) analysis of the peptides was performed using the Chirascan Circular Dichroism Spectrometer (Applied Photophysics Limited, U.K.). Briefly, the CD spectra of CWR11 were generated in three environments: (i) deionized water, (ii) phosphate buffered saline (PBS) solution, and (iii) 20 mM sodium dodecyl sulfate (SDS) solution. Each spectrum was obtained over a wavelength range of 190−260 nm with an interval of 0.5 nm, at a speed of 1.0 nm s^{-1}, and a bandwidth of 1.0 nm. Three scans were conducted and averaged to obtain each spectrum, which were presented as mean residue ellipticity, θ (degrees cm^2 mol^{-1}). Baseline scans were obtained for the respective buffer and micelles only, and subtracted from the respective CD spectra generated in the presence of the peptide. All spectra were recorded at a fixed peptide concentration of 300 μM. Peptide secondary structure compositions under different physicochemical environments were determined by spectra deconvolution using the CDNN software.

2.5. Membrane Permeabilization Studies. *2.5.1. Field-Emission Scanning Electron Microscopy (FESEM).* The peptide at the previously determined MIC concentration was incubated with *E. coli*, *S. aureus*, and *P. aeruginosa* for 1 h at 37.0 °C. After incubation, the bacteria cells were fixed with 2.5% glutaraldehyde and incubated for 16 h on glass sides (24 mm × 50 mm). The glass slides were rinsed with 10 mM phosphate buffer (pH 7.0) and dehydrated through a graded ethanol series (25%−100%). The slides were dried under constant airflow for 15 min, and coated with platinum for 100 s at 10 mA. The bacterial membrane morphologies were imaged with field-emission scanning electron microscopy (FESEM) (Model JSM-6700F field-emission electron microscope, JEOL, Japan).

2.5.2. 1-N-phenylnapthylamine (NPN) Uptake Assay. The extent of peptide-induced outer membrane permeabilization was determined using the NPN assay.[13] Briefly, *E. coli* strains were grown overnight, reinoculated, and grown to an outer diameter of OD_{600} = 0.5. Bacterial cells were washed three times with 10 mM phosphate buffer (pH 7.0), before resuspension in the same buffer to attain an OD_{600} value of 0.5. Then, 1.0 mL of the bacterial suspension was added to various concentrations of peptide (0−14 μM), followed by 20.0 μL of 0.5 mM NPN solution to attain a final NPN concentration of 10 μM. Fluorescence measurements of the samples were performed using a fluorescence spectrophotometer (Model LS5, Perkin−Elmer, Eden Prairie, MN, USA) at an excitation wavelength of 350 nm, an emission wavelength of 420 nm, and a slit width of 5.0 nm. Fluorescence measurements were taken in triplicate and averaged.

2.5.3. Propidium Iodide (PI) Fluorescence Assay. The membrane permeabilization ability of the peptide CWR11 was investigated by fluorescence measurements of DNA-binding propidium iodide in the presence of bacteria cells and the peptide. *E. coli* cells were grown overnight in MH medium and reinoculated in a fresh medium to obtain an OD_{600} value of 0.5. Cells were harvested and subjected to washing three times with 10 mM phosphate buffer (pH 7.0). Washed bacterial cells were resuspended in 10 mM phosphate buffer (pH 7.0) to obtain a final concentration of 1×10^8 CFU/mL. Then, 1.0 mL of the *E. coli* cells was withdrawn and mixed with 20.0 μL of propidium iodide (1.0 μg/mL). The bacterial suspension was then added to sequential peptide concentrations ranging from 1/8 to 1× MIC). Fluorescence measurements were measured using a fluorescence spectrophotometer (Model LS5, Perkin−Elmer, Eden Prairie, MN, USA) with excitation and emission wavelengths set at 520 and 620 nm, respectively.

2.6. CWR11 Immobilization on Polydimethylsiloxane (PDMS) Slides. *2.6.1. Synthesis of P Polydimethylsiloxane (PDMS) Slides.* Polydimethylsiloxane (PDMS) polymer was synthesized using a kit (184 elastomer kit, Dow Corning, USA), according to the manual's instructions in 90-mm Petri dishes and subsequently cut into 1.0 cm × 1.0 cm slides for peptide immobilization studies.

2.6.2. Plasma and UV Polymerization of PDMS Slides with Allyl Glycidyl Ether (AGE). Allyl glycidyl ether (AGE) polymer brush synthesis on the PDMS slides was performed by continuous plasma activation and UV treatment with an AGE monomer. Briefly, 1 cm^2 PDMS slides were rinsed with acetone to remove any impurities on the surface, and subjected to plasma treatment for surface activation. Plasma activation was conducted using the March PX-500 Plasma treatment system (Nordson, Westlake, OH, USA). Continuous plasma was performed at 300 W for 10 min in the presence of inert argon gas. The activated PDMS slides were successively immersed in 100% (v/v) AGE, and subjected to UV radiation for 60 min. The AGE-tethered slides (PDMS−AGE) were washed with distilled water (three times, 5 min each time with 5.0 mL of distilled water).

2.6.3. Attachment of Polyethylene Glycol (PEG) Spacer to PDMS-AGE Slide. Maleimide−polyethylene glycol (PEG)−amine heterobifunctional PEG (NH_2−PEG−Mal) (3.4 kDa) was purchased from Nanocs (USA). NH_2−PEG−Mal was dissolved in deionized water to a final concentration of 5.0 mg/mL. The activated surface of polydimethylsiloxane (PDMS)−AGE slides were covered with the PEG solution, and the slides together with the solution were incubated at 25.0 °C for 16 h. The PEG-grafted PDMS slides (PDMS−AGE−PEG) were then washed in deionized water (three times, 5 min each time with 5.0 mL of distilled water).

2.6.4. Cross-Linking of CWR11 to AGE-Modified PDMS Surface via Sulfhydryl Chemistry. Peptide cross-linking was performed using the sulfhydryl chemistry between the peptide and maleimide group derived from the PEG-functionalized PDMS slides based on a reported protocol.[14] Briefly, the PDMS−AGE−PEG slides were immersed in 2.0 mg/mL peptide solution and the reaction was allowed to occur at 25.0 °C for 16 h. After incubation, the peptide-tethered PDMS slides (PDMS−AGE−PEG−CWR11) were rinsed thoroughly with 10 mM

phosphate buffer (five times, 5 min each time with 5.0 mL of 10 mM phosphate buffer), followed by deionized water (five times, 5 min each time with 5.0 mL of distilled water) to remove any unbound peptides. The slides were dried in a nitrogen stream and stored at −20.0 °C for further use.

2.7. Surface Characterization of CWR11-Immobilized PDMS Slides. *2.7.1. Contact Angle Measurement.* As a quality control measure, static water contact angle measurements of each sample were performed with a dynamic contact angle analyzer (Fta 200, Fta, U.K.). 5.0 μL water droplet was introduced onto the respective PDMS surfaces and digital images were taken with a high-magnification imaging lens (Navitar, Rochester, NY, USA). Contact angle quantitation was performed using the Fta32 software.

2.7.2. X-ray Photoelectron Spectroscopy (XPS). XPS analysis was performed to determine the elemental atomic percentage on the surface of the peptide-immobilized PDMS slide. High-resolution spectra of carbon, nitrogen, oxygen, and silicon were obtained individually using an X-ray photoelectron spectrometer (Axis-ULTRA, Kratos), installed with an Al Kα radiation source (10.0 mA, 15.0 kV), and analyzed to determine the respective elemental ratio.

2.7.3. Energy-Dispersive X-ray Spectroscopy (EDS). Attachment and distribution of peptides immobilized on the PDMS surface was analyzed using EDS (FESEM, using a JEOL Model JSM-6700F field electron microscope, Japan). The elemental content was quantified using the Analysis Station software.

2.7.4. Attenuated Total Reflectance–Fourier Transform Infrared (ATR-FTIR) Spectroscopy. Peptide-immobilized PDMS samples were subjected to ATR-FTIR analysis to verify the presence of amide bonds on the surface. The spectrum was recorded on a Thermo Nicolet 5700 FT-IR spectrometer (Thermo Fisher Scientific, USA) equipped with a Diamond ATR accessory unit. PDMS–AGE–PEG–CWR11 and PDMS–AGE–PEG slides were placed on the surface of the ATR unit. Each spectrum was recorded at 25.0 °C from 400 cm^{-1} to 4000 cm^{-1} over 32 scans.

2.7.5. Peptide Concentration Determination by Sulfosuccinimidyl-4-o-(4,4-Dimethoxytrityl) Butyrate (Sulfo-SDTB) Spectrophotometric Assay. Immobilized peptide concentration was determined using the sulfosuccinimidyl-4-*o*-(4,4-dimethoxytrityl) butyrate (Sulfo-SDTB) spectrophotometric assay (Bioworld, USA) according to the suppliers' instruction manual. Briefly, 3.0 mg of Sulfo-SDTB was dissolved in 1.0 mL of dimethylformamide (DMF), and topped with sodium bicarbonate solution (pH 8.5, up to 50.0 mL). To the peptide-immobilized samples, 1.0 mL of the Sulfo-SDTB solution and 1.0 mL of sodium bicarbonate was added, and incubated for an hour at 25 °C. The samples were subsequently washed twice in 5.0 mL of distilled water, and immersed in 2.0 mL of perchloric acid for 30 min. Upon incubation, 500 μL of the perchloric acid was removed and the absorbance at 498 nm was measured.

The amount of amine groups on the surface of each sample was quantified using the Beer–Lambert law with an extinction coefficient of 70 000 M^{-1} cm^{-1}. The amount of peptides immobilized on each sample was calculated by calibration against the predicted number of amines per peptide.

2.8. Antimicrobial Activity Determination of CWR11-Immobilized PDMS Slide. The antimicrobial activity of the PDMS–AGE–PEG–CWR11 slides was determined using an adapted ISO protocol (ISO 22196).[15] Briefly, *E. coli* bacterial strains were cultivated in a MH medium, for 16 h at 37.0 °C. The overnight bacterial suspension was then reinoculated in a fresh medium and grown to OD_{600} = 0.5. The test inoculum was diluted to a final concentration of 1×10^6 CFU/mL. 50.0 μL of the bacterial suspension was then spread over each PDMS–AGE–PEG–CWR11 slide. The inoculated slides were incubated at 37.0 °C for 3 h, under 70 rpm shaking conditions. 5.0 μL of the inoculum was withdrawn from each PDMS slide and plated for colony counts. The same PDMS slide, with the remaining inoculum, was then immersed in 2.0 mL of fresh MH medium and incubated at 37.0 °C, 250 rpm for 18 h to determine the antimicrobial activity of the slides. The protocol was repeated in triplicate for *E. coli*, *S. aureus*, and *P. aeruginosa*.

2.9. Stability Determination of Immobilized Peptides. To determine the stability of the PDMS-immobilized peptides, a leaching assay was conducted using a reported protocol.[14] Peptide-immobilized PDMS slides were immersed in distilled H_2O for 1–3 days. Peptide stability was investigated by antibacterial testing, as described in Section 2.8.

2.10. Antibiofilm Activity of Peptide-Immobilized PDMS Slides. *2.10.1. Crystal Violet (CV) Staining of Biofilm.* Each PDMS slide was rinsed with 70% ethanol (v/v) and dried. The PDMS slides were secured to the bottom of the wells, in a 24-well plate. GFP-*P. aeruginosa* (1×10^8 CFU) in 1 mL of biofilm-promoting medium (BPM) was added to each well. BPM with no bacteria was added as control. After 24 h of incubation at 37 °C, planktonic bacteria were removed and the wells, together with the PDMS slides, were washed 5 times with deionized water. 1.2 mL of 0.1% crystal violet stain was added to the wells and incubated for 15 min at 25.0 °C, followed by washing with distilled water. The wells and PDMS slides were dried in a 37.0 °C incubator.

The crystal violet stain on PDMS slides were solubilized in 200 μL of 30% acetic acid (v/v) for 15 min. One hundred microliters (100 μL) of solubilized crystal violet was added to 100 μL of 30% acetic acid in 96-well plate wells, and the amount of solubilized crystal violet was measured by their absorbance at 550 nm.

2.10.2. Live/Dead Biofilm Staining. Overnight *E. coli* culture was diluted in a MH broth to a final concentration of 1×10^8 CFU/mL. PDMS–AGE–PEG–CWR11, PDMS–AGE–PEG, and PDMS slides were immersed in 2.0 mL of a bacteria suspension for 5 days to ensure complete biofilm formation. After 5 days, planktonic bacteria were removed by briefly rinsing the respective slides with PBS. The slides were then dried and stained with a LIVE/DEAD kit (Invitrogen Molecular Probes, USA) according to the manufacturer's instructions. The samples were examined with a LSM710 META confocal microscope (Carl Zeiss, Germany). For detection of SYTO 9 (green channel), the excitation wavelength was set at 488 nm. For PI detection (red channel), an excitation wavelength of 561 nm was utilized. Images at both excitation wavelengths were captured and processed using the Zen 2009 software.

2.11. Cytotoxicity Assay. The hemolytic activities of the immobilized peptides against human erythrocyte cells were studied using a method adapted from Shai et al.[16] Fresh human red blood cells (hRBC) were rinsed and washed three times with PBS, centrifuged for 10 min at 900 g, and resuspended in PBS to a final erythrocyte concentration of 5.0% (v/v). The peptide-immobilized and untreated PDMS slides were each immersed in 2.0 mL hRBC solution and incubated for 1 h at 37.0 °C, with agitation at 100 rpm. Upon incubation, the samples were centrifuged at 1500 g for 5 min. Hemoglobin release was measured by absorbance measurement of the supernatant at 540 nm. Controls for 0% hemolysis and 100% hemolysis were obtained by suspending hRBC in PBS and 1% Triton X, respectively.

Methyl tetrazolium (MTT) assay was also performed to determine cell viability and proliferation capability of human aorta smooth muscle cells, CC-2571 (Lonza, USA) on the peptide-immobilized slides. The PDMS–AGE–PEG–CWR11 slides were cut into 5-mm-diameter disks and placed in 70% ethanol for 24 h for sterilization, followed by incubation in PBS for 16 h in 96-well culture plate. Smooth muscle cells (0.5×10^5 cells/cm^2) and culture medium were then added to the respective wells containing the slides. The cells were allowed to grow for 7 days, coupled with a culture medium change every 2 days. On day 1, 2, and 7, mammalian cell culture from the wells containing peptide-treated and untreated PDMS slides were withdrawn and placed in a 96-well tissue culture polystyrene (TCPS) plate. MTT solution (5 mg/mL, 100 μL) was incubated with the respective mammalian cell culture at 37 °C for 4 h, followed by DMSO (200 μL) addition and shaking for 30 min. Absorbance measurement at 490 nm was conducted using a microplate spectrophotometer (Bio-Rad, USA).

Viability of smooth muscle cells upon 7 days of incubation with peptide-immobilized and control PDMS slides, was examined with the LIVE/DEAD Assay. Cells were stained with LIVE/DEAD Assay reagent (Invitrogen, USA) and incubated at 25 °C for 45 min.

Morphology of the cells was observed with an inverted optical microscope (Zeiss, Germany).

2.12. Statistical Analysis. All experiments were conducted in triplicate (except crystal violet staining of biofilm (duplicate)). Mean and standard deviations were calculated for all repeated measurements. Statistical analysis was performed with SPSS for Mac software, version 21.

3. RESULTS

3.1. Activity and Structural Studies of Soluble CWR11. The peptides' MICs against three target pathogens were determined by performing a broth microdilution assay.[12] Table 1 shows that the engineered peptide (WR11), with amino acid sequence WFWKWWRRRRR-NH_2, possessed low MICs of 3.1 μM, 1.7 μM and 4.6 μM toward *E. coli*, *S. aureus*, and *P. aeruginosa*, respectively. In view of the objective to immobilize the peptide on a surface via specific sulfhydryl coupling, N-terminal cysteine was performed on WR11 to yield CWR11 (CWFWKWWRRRRR-NH_2), which resulted in a slight increase in the MIC values. The addition of 150 mM NaCl also slightly affected the antimicrobial activity of CWR11, as reflected by a slight increase in MIC values to 7.3 μM, 4.7 μM, and 8.7 μM against the respective pathogens. However, CWR11 MIC values remain below 10.0 μM and demonstrate retention of excellent antimicrobial potency, even in the presence of salt.

Table 1. MICs of Wild Type Peptide, WR11, and CWR11 against *E. coli*, *S. aureus*, and *P. aeruginosa*

	Minimum Inhibitory Concentration (μM)			
			CWR11	
	Jelleine I	WR11	no salt	150 mM NaCl
E. coli	2.6	3.1 ± 0.6	5.2 ± 0.5	7.3 ± 0.0
S. aureus	10.5	1.7 ± 0.0	2.5 ± 0.0	4.7 ± 0.9
P. aeruginosa	10.5	4.6 ± 0.2	5.5 ± 0.0	8.7 ± 1.2

Secondary structure analysis of CWR11 by CD spectroscopy in the presence of deionized water, PBS and 20mM SDS suggests that CWR11 adopts a mixed α-helix and β-sheet conformation in deionized water (Figure 1), with two weak troughs observed at 202 and 220 nm, as well as a peak at 190 nm. In PBS, the troughs shifted to 205 and 222 nm, while in the presence of 20 mM SDS, a further shift of the troughs to 207 and 218 nm were observed, with increased intensity. Spectra deconvolution indicates an enhanced peptide helicity in the presence of PBS and membrane mimicking SDS, where an estimated increase in helicity from 40.9% (in deionized water) to 96.2% and 98.4% in PBS and 20 mM SDS, respectively, was attained.

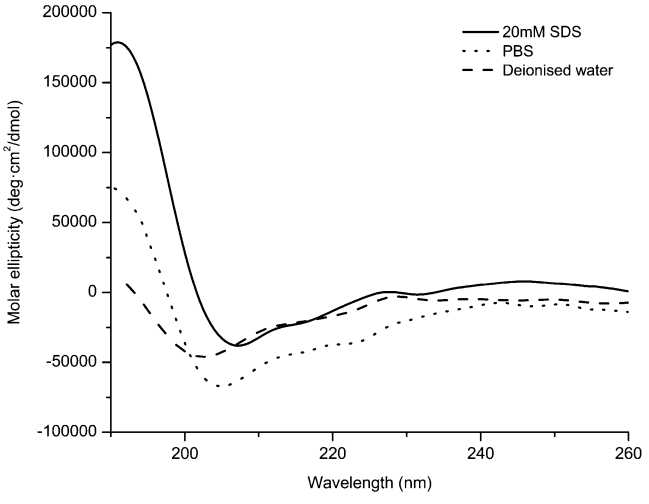

Figure 1. Circular dichroism spectra of CWR11 peptide in (- - -) deionized water, (···) PBS buffer, and (—) 20 mM SDS. Peptide concentrations are fixed at 300 μM.

3.2. Membrane Permeabilization Studies. The effect of CWR11 on bacteria membrane morphological change was studied by FESEM. Figure 2A shows the electron microscopy images of CWR11-treated and untreated bacteria cells. Heavily crinkled outer membrane coupled with formation of bulbous structures on the peptide-treated cells confirmed the membrane

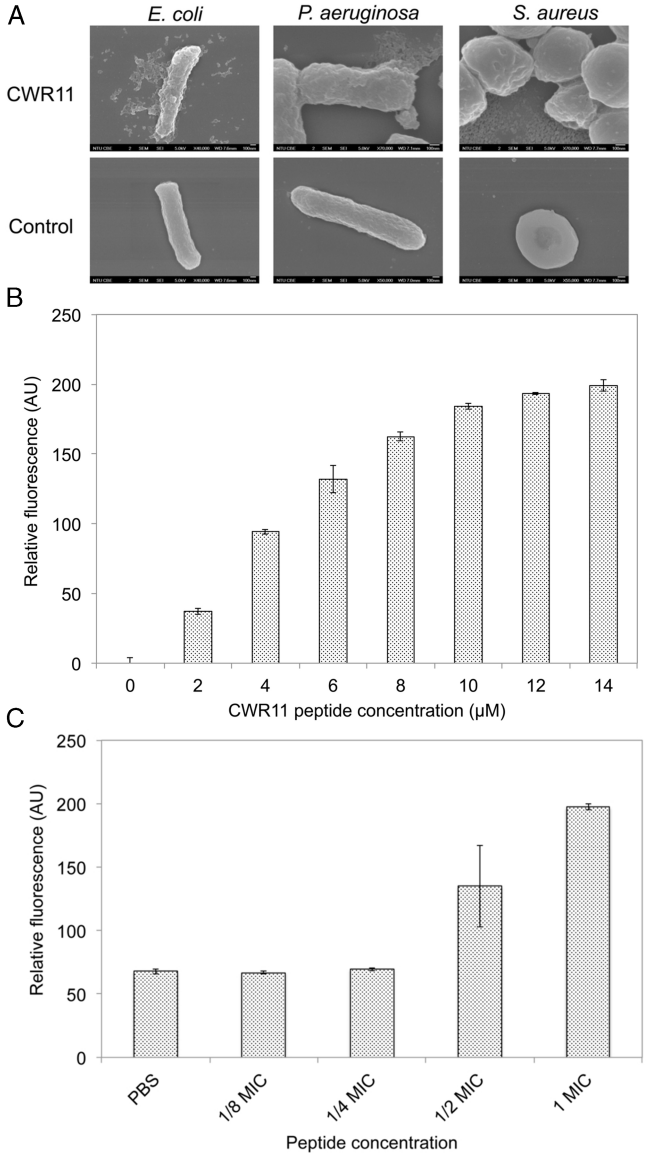

Figure 2. In vitro characterization of CWR11 membrane disruption potential. (A) FESEM images of *E. coli*, *P. aeruginosa*, and *S. aureus* after treatment with CWR11 (top panel) and untreated controls (bottom panel). (B) Outer membrane permeabilization studies by NPN fluorescence assay. (C) DNA intercalation with PI dye to study membrane permeabilization effect of C-WR11.

dx.doi.org/10.1021/am401629p | ACS Appl. Mater. Interfaces 2013, 5, 6412−6422

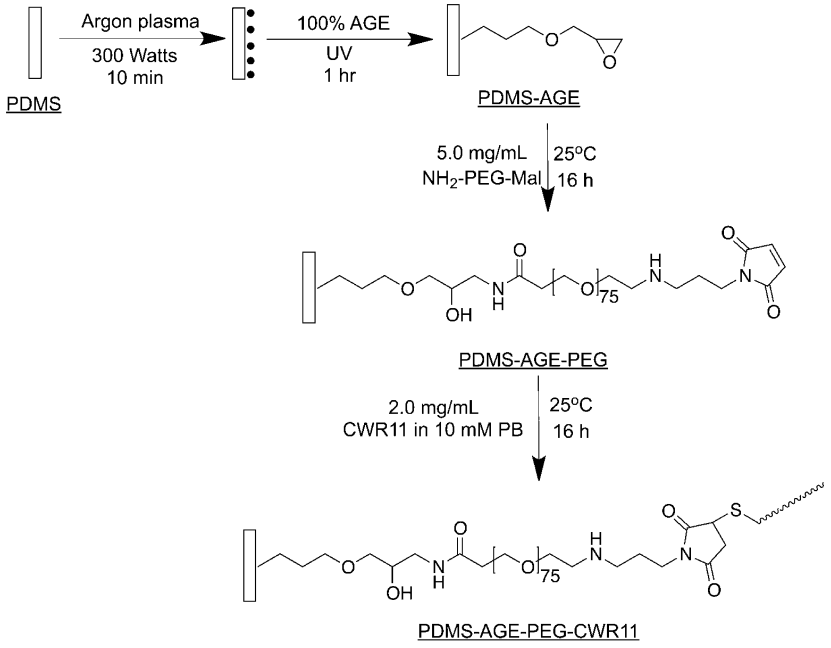

Figure 3. Schematic of CWR11 peptide immobilization chemistry on PDMS surface. The PDMS surface is first activated by exposure to an argon plasma, followed by grafting of AGE brushes and peptide sulfhydryl coupling via the NH_2−PEG−Mal linker.

disruption ability of CWR11. The outer membrane perturbation ability of CWR11 was further confirmed by the NPN uptake assay. NPN is a chemical compound that fluoresces weakly in an aqueous environment, but, under hydrophobic conditions, gives off a strong fluorescence at 350 nm excitation.[17] Figure 2B shows an increase in NPN fluorescence with increasing CWR11 concentrations, when incubated with *E. coli*. At a peptide concentration above 10 μM, there was no increase in fluorescence with further increase in peptide concentration, indicating that all the available surface area of the cell membrane had been permeabilized by the peptide.

The membrane permeabilization ability of CWR11 was also assayed by studying DNA binding of PI.[18] Upon binding to DNA, PI fluoresces strongly at an excitation wavelength of 520 nm. Figure 2C shows that the PI fluorescence reading increases with increasing peptide concentration, indicating the cytoplasmic membrane disruption ability of CWR11, which leads to the diffusion of PI into the bacteria's cytoplasm.

3.3. CWR11 Immobilization on PDMS Surface and Surface Characterization by Contact Angle, ATR-FTIR, EDS, XPS Analyses and Sulfo-SDTB Spectrophotometric Assay. Following confirmation of the excellent antimicrobial properties of CWR11, we proceeded to develop a peptide immobilization platform on a PDMS surface. Figure 3 provides a schematic that illustrates the steps involved in the immobilization of CWR11 on PDMS surface. One-square-centimeter (1 cm^2) PDMS slides were exposed to continuous plasma treatment to activate the surface with reactive free radicals. The activated surfaces were exposed to AGE under UV. The exposed epoxy groups on the AGE-immobilized PDMS slides were allowed to react with bifunctional PEG moieties (NH_2−PEG-Mal), where the amine on the PEG molecule would react with the epoxy group on the PDMS surface to form a hydroxyl group and secondary amine. The exposed maleimide group is subsequently available for sulfhydryl coupling with the cysteine residue of the CWR11 peptide.

Contact angle measurements were performed to assess the change in surface hydrophilicity of the AMP-immobilized PDMS slides (see Table 2). PDMS is inherently hydrophobic,[19]

Table 2. Contact Angle Measurement of Deionized Water on Treated and Untreated PDMS Surfaces

	contact angle (°)
PDMS	105.76 ± 5.62
PDMS−AGE	42.96 ± 5.10
PDMS−AGE−PEG	54.20 ± 0.72
PDMS−AGE−PEG−CWR11	67.01 ± 0.98

as shown by a high contact angle of 106°. Plasma activation and polymerization of AGE onto the PDMS surface drastically enhanced the hydrophilicity of the PDMS surface, as shown by a reduction in contact angle to 43°. Subsequent attachment of PEG moieties and peptide increased surface hydrophobicity, as indicated by an increase in contact angle by 8° and 13°, respectively. This is attributed to the hydrophobic carbon backbone of the PEG and peptide.

Figure 4A shows the ATR−FTIR spectrum obtained for PDMS−AGE−PEG−CWR11 and PDMS−AGE−PEG. For PDMS−AGE−PEG−CWR11, peaks can be observed at 1653 and 1558 cm^{-1}, which are representative of amide I and amide II bands; these were absent in the PDMS−AGE−PEG samples. The presence of these bands confirmed that peptide immobilization on the slides was successful.

XPS analysis is a highly sensitive tool that is used to determine atomic percentages of elements on surfaces.[15] Measurement of nitrogen atomic percentages could provide qualitative and quantitative indications of PEG and peptide attachment to the PDMS surfaces. The XPS spectrum indicates the appearance of peaks at 400 eV for PDMS−AGE−PEG and PDMS−AGE−PEG−CWR11 samples (Figure 4B), albeit at different intensity. The N1s peak for PDMS−AGE−PEG corresponded to a nitrogen content of 1.1 at. %, while that in PDMS−AGE−PEG−CWR11 corresponded to 6.1 at. %. As

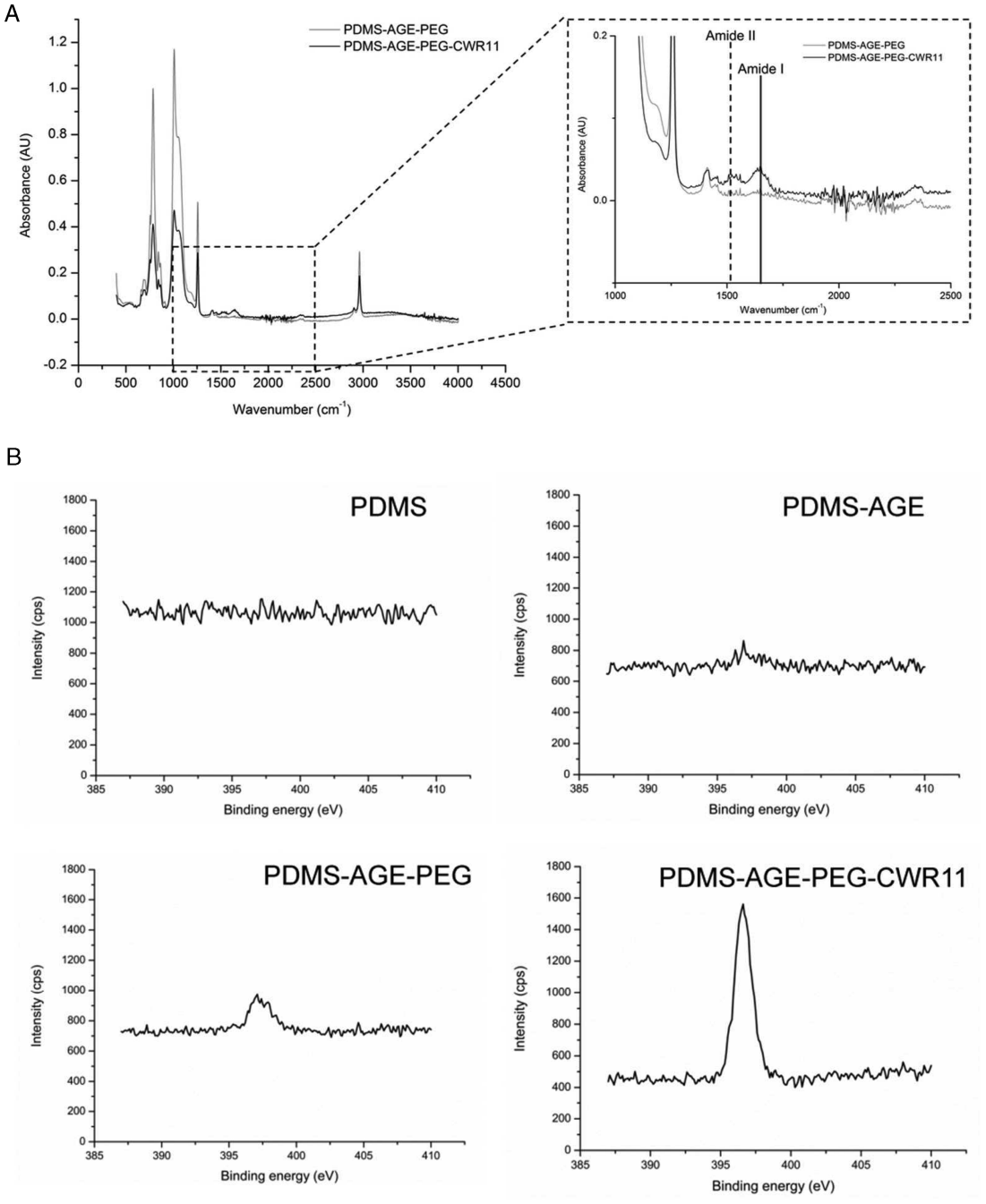

Figure 4. Surface characterization of CWR11-immobilized PDMS slides: (A) ATR−FTIR spectrum for determination of amide bonds in PDMS−AGE−PEG (gray) and PDMS−AGE−PEG−CWR11 (black) slides; (B) XPS analysis of untreated and treated PDMS at different stages. High-resolution XPS spectra of the N1s region for PDMS, PDMS−AGE, PDMS−AGE−PEG, and PDMS−AGE−PEG−CWR11.

expected, PDMS−AGE−PEG−CWR11 showed a higher nitrogen atomic percentage, compared to PDMS−AGE−PEG slides, because of the higher content of amine groups present within the peptide sequence.

EDS was employed to further confirm peptide immobilization by sulfur content measurement. Based on the library from the Analysis Station software, a peak specific to sulfur can be identified for the peptide-immobilized sample, which was absent for the other control samples, i.e., PDMS, PDMS−AGE, and PDMS−AGE−PEG slides (data not shown). A quantification analysis of the sulfur atomic percentage indicates that ∼1.1% of sulfur was present on PDMS−AGE−PEG−CWR11.

Sulfo-SDTB was used to quantify the amount of free amine group on the peptide-immobilized PDMS surface. Under acidic conditions, 4,4-*o*-dimethoxytrityl ions would be released from the surface-bound sulfo-SDTB, and quantitated by absorbance measurement at 498 nm.[20] Using this method, the amount of immobilized CWR11 on the PDMS surface was estimated to be $0.8 \pm 0.2\ \mu g/cm^2$ (or $4.16 \pm 1.04 \times 10^{-4}\ \mu mol/cm^2$).

3.4. Antimicrobial Activity Determination of CWR11-Immobilized PDMS. To determine the antimicrobial potency of the peptide-immobilized PDMS surface, 50 μL of 1×10^6 CFU/mL of bacterial inoculum was spread onto the slide surface and incubated at for 3 h. Five microliters (5 μL) of the total bacterial inoculum from the surface antimicrobial activity

dx.doi.org/10.1021/am401629p | ACS Appl. Mater. Interfaces 2013, 5, 6412−6422

Table 3. Antimicrobial Activity of CWR11-Immobilized PDMS Slides against *E. coli*, *S. aureus*, and *P. aeruginosa*[a]

	E. coli		*S. aureus*		*P. aeruginosa*	
initial bacterial concentration (CFU/mL)	colony count (CFU)	inhibition (%)	colony count (CFU)	inhibition (%)	colony count (CFU)	inhibition (%)
10^6	0 ± 0	99.9 ± 0.0	0 ± 0	99.9 ± 0.0	0 ± 0	99.9 ± 0.0

[a]CFU counts after incubating 10^6 CFU/mL of respective bacteria suspension with a PDMS−AGE−PEG−CWR11 slide.

assay on the PDMS−AGE−PEG−CWR11 slides was withdrawn and spread on agar plates, followed by CFU determination. The result shows that the peptide-immobilized PDMS slides were highly bactericidal, with no observable CFU growth on the agar plates (see Table 3). Subsequent immersion of the same peptide-immobilized PDMS slides containing the remaining bacterial inoculum, in fresh medium, showed comparable optical density readings to blank medium, while the control (PDMS) slide supported bacteria growth (see Figure 5). This result confirms that the antimicrobial activity of

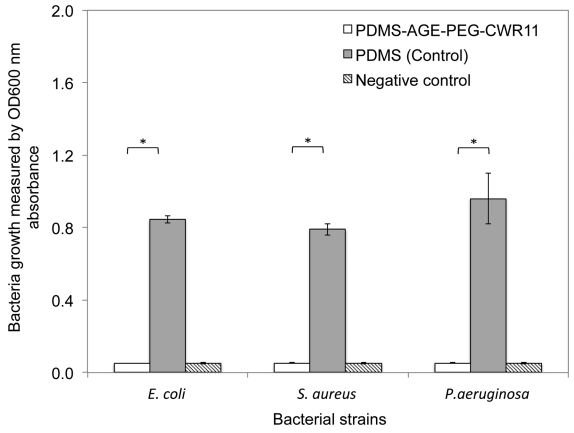

Figure 5. Antimicrobial activity of CWR11-immobilized PDMS slides against *E. coli*, *S. aureus*, and *P. aeruginosa*. Optical density measurements of fresh MH medium after overnight incubation with PDMS slides containing remaining bacterial suspension after performing CFU counts.

the peptide was retained after immobilization, with 99.9% inhibition of bacterial growth. This observation was consistent for all three bacterial strains.

3.5. Stability of CWR11-Immobilized PDMS Slides. To investigate the stability of immobilized CWR11, PDMS−AGE−PEG−CWR11 slides were subjected to soft cleaning conditions (i.e., overnight immersion in water), followed by an antimicrobial assay. Figure 6 shows the CFU counts obtained after immersion of PDMS−AGE−PEG−CWR11 slides in distilled water, which indicated that the slides retained antimicrobial potency and completely inhibited *E. coli* growth up to at least 3 days.

3.6. Antibiofilm Determination of Immobilized CWR11. Using crystal violet staining to determine biofilm formation on surfaces,[21] it was observed that the PDMS−AGE−PEG−CWR11 slides showed a much lower crystal violet staining intensity in contrast to the negative control, PDMS−AGE−PEG (see Figure 7A). An optical density measurement of the crystal violet solution quantitatively showed that biofilm formation on PDMS−AGE−PEG−CWR11 was significantly reduced, compared to the control slide (Figure 7B), which indicates the potent antibiofilm capability of the peptide-tethered surface.

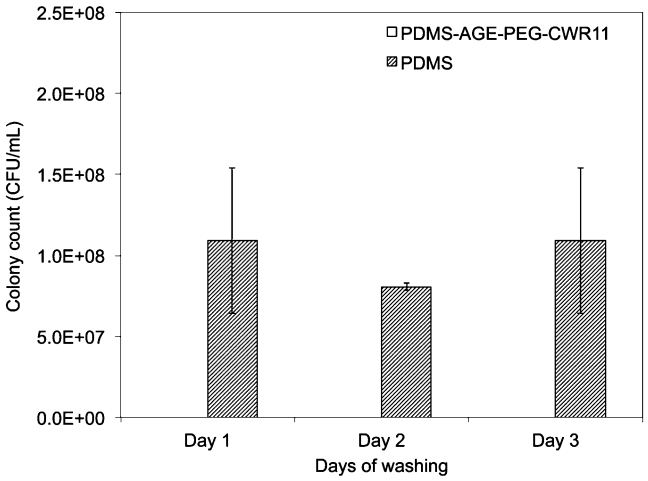

Figure 6. Antibacterial activity determination (by CFU counting) of PDMS−AGE−PEG−CWR11 after immersion in deionized water for 1−3 days.

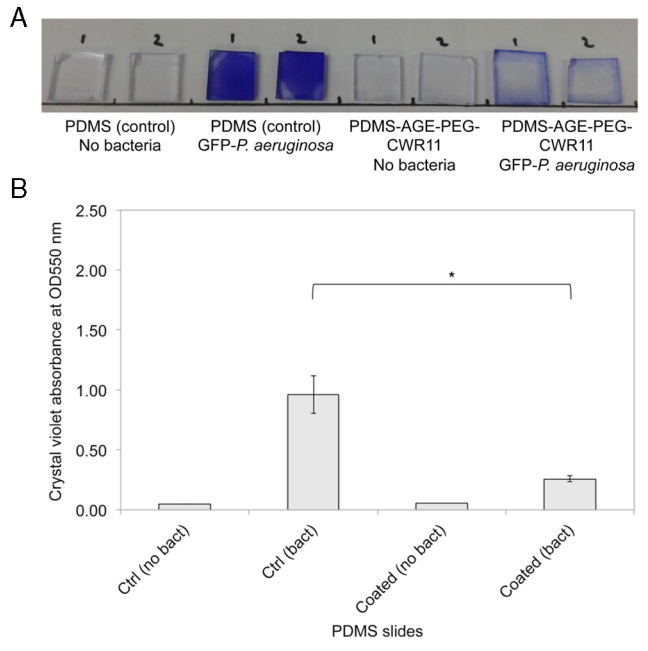

Figure 7. Assessment of biofilm formation via crystal violet staining: (A) treated and untreated PDMS samples and controls stained with crystal violet upon incubation with *P. aeruginosa* for 24 h to allow substantial biofilm formation; (B) optical density measurement at 550 nm of the crystal violet solution.

Figure 8 shows the confocal microscopy image of *E. coli* biofilm, post-staining with LIVE/DEAD dyes. The high fluorescence observed in the unmodified PDMS slides indicates the presence of a large number of cells attached on the slide surface. Corresponding PI staining showed that most of the cells were viable, suggesting the presence of extensive biofilm on the untreated PDMS surface. The PEG-functionalized

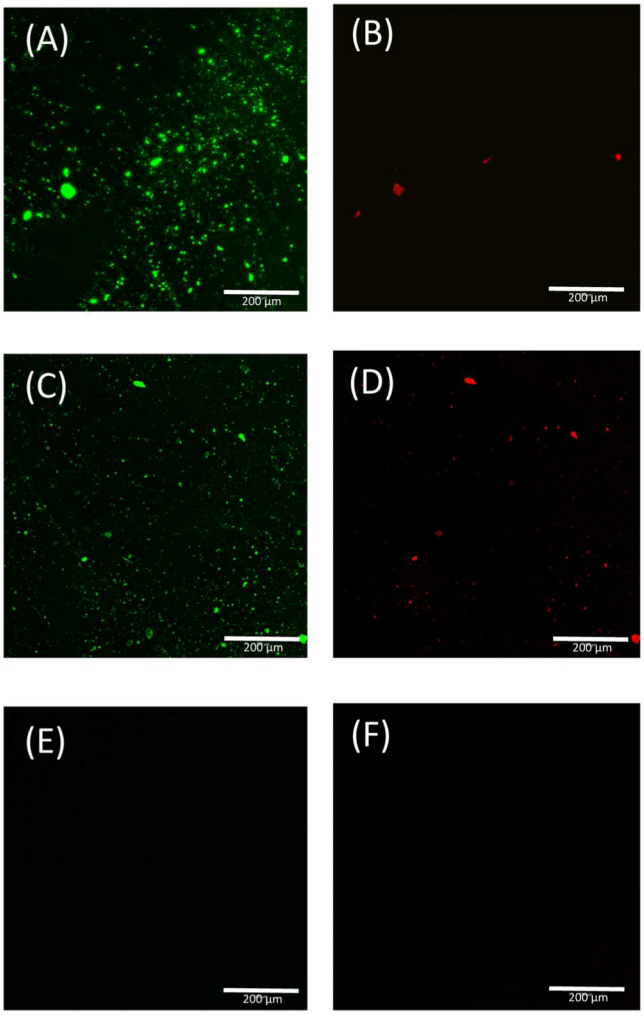

Figure 8. *E. coli* biofilm formation after 5 days of growth on CWR11-immobilized and untreated PDMS slides. The biofilms were stained with LIVE/DEAD assay and imaged with confocal laser scanning microscopy. Staining of untreated PDMS slides with (A) Syto 9 and (B) PI, PDMS−AGE−PEG slides with (C) Syto 9 and (D) PI, and PDMS−AGE−PEG−CWR11 with (E) Syto 9 and (F) PI.

PDMS slides had a reduced amount of attached cells, which is consistent with PEG's anti-"cell adhesion" properties. The PDMS−AGE−PEG−CWR11 slides showed complete eradication of bacteria attachment, since no viable or dead cells could be observed on the slide surface.

3.7. Cytotoxicity Assay of Immobilized CWR11. PDMS−AGE−PEG−CWR11 slides incubated in 2.0 mL 5.0% erythrocyte solution showed no statistical difference in hemolytic activity, compared to the untreated PDMS control (Figure 9A). No significant hemolytic activity was detected from the immobilized peptides after an hour of incubation with red blood cells, which indicates that the amount of peptide impregnated on the PDMS slides were not toxic to red blood cells.

Cytotoxicity of PDMS−AGE−PEG−CWR11 slides against mammalian smooth muscle cells (SMCs) was determined using the MTT assay. The peptide-immobilized PDMS slide did not display toxicity to mammalian cells. Upon incubation with the PDMS−AGE−PEG−CWR11 slides, the SMCs continued to grow, as indicated by an increase in MTT absorbance from day 1 to day 7. No statistical difference in MTT absorbance was

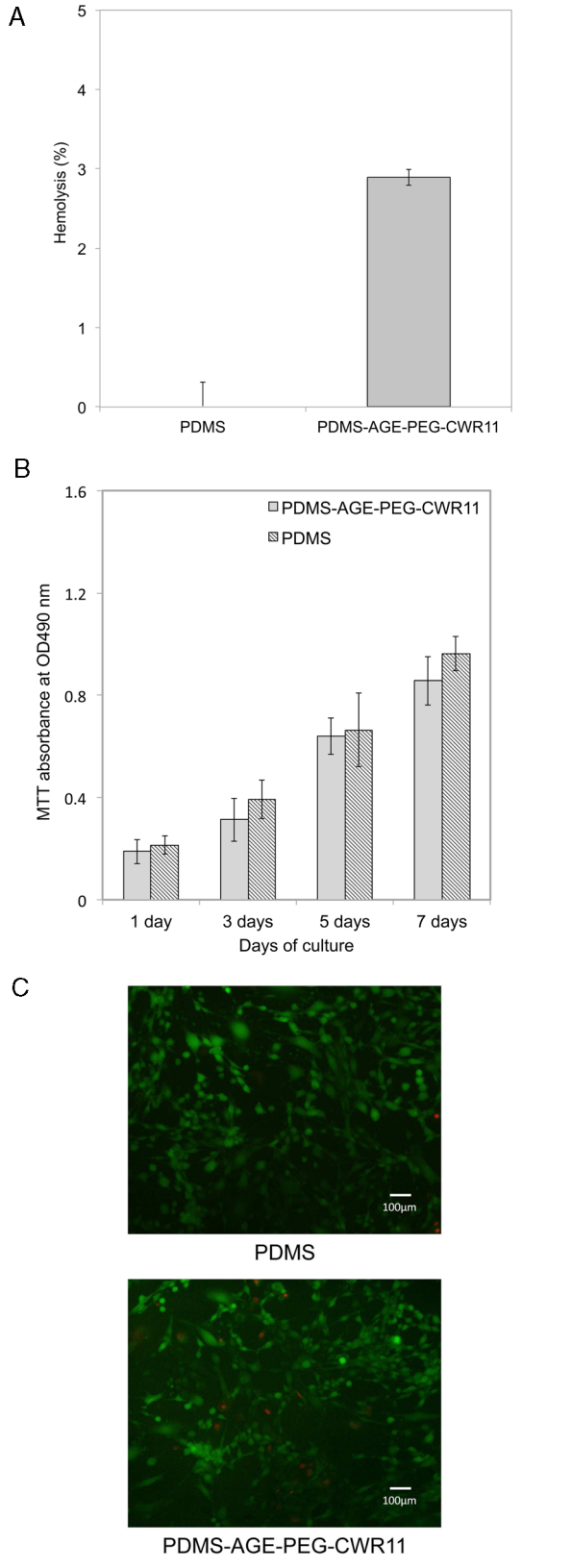

Figure 9. (A) Cytotoxicity studies of PDMS−AGE−PEG−CWR11 against human erythrocyte cells. (B) MTT assay of mammalian smooth muscle cells incubated with PDMS−AGE−PEG−CWR11. (C) Smooth muscle cell viability assay on PDMS and PDMS−AGE−PEG−CWR11 slides.

dx.doi.org/10.1021/am401629p | ACS Appl. Mater. Interfaces 2013, 5, 6412−6422

observed between the untreated PDMS control and the peptide-immobilized slides. LIVE/DEAD assay of the mammalian cells exposed to PDMS−AGE−PEG−CWR11 showed that the majority of the mammalian cells remained viable up to 7 days of incubation with the slide (see Figure 9C).

4. DISCUSSION

4.1. Peptide Design and Characterization. Several cycles of systematic amino acid substitution of R and W residues were performed on the wild type Jelleine-I peptide to generate a *denovo* arginine- and tryptophan-rich peptide (WR11) having an optimal peptide charge to hydrophobic ratio, leading to maximum antimicrobial potency. Tryptophan was chosen to modulate the peptide's hydrophobicity due to its preference for membrane−water interfacial region,[8] which is likely to augment the insertion of peptide into the hydrophobic core of the phospholipid bilayer membrane. Substitution with arginine residues was intended to enhance electrostatic interaction with the negatively charged bacterial membrane. In contrast to lysine, arginine side chains are able to form hydrogen bonds with surrounding water molecules while engaged in cation−π interaction with tryptophan.[6,22] This cation−π interaction with tryptophan, coupled with the formation of multiple hydrogen bonds with water molecules, makes the entry of arginine residues into the hydrophobic bilayer more energetically favorable.

The most potent engineered variant, WR11, possessed a net charge of +7, which is contributed by the high arginine content and amidation of the C-terminal. WR11 exhibited significantly lower MIC toward three species of bacteria, compared to the parent peptide. The peptide was particularly potent against gram-positive *S. aureus* (MIC of 2.6 μM), which is a microbe that is prevalent in community- and hospital-acquired infection; it posseses strong resistance against conventional antibiotics and some natural AMPs.[23] The superior potency of WR11 merits its further study as an antimicrobial coating agent for biomedical devices. N-terminal cysteine modification of the synthetic AMP sequence was performed to provide greater ease for further covalent immobilization. The addition of an extra amino acid residue at the N-terminal of WR11 did not significantly increase the peptide's MIC values. In the presence of physiological salt concentration, CWR11 retained its potent antimicrobial ability, maintaining MICs below 10.0 μM against all three pathogens. These properties render CWR11 superior in contrast to many antimicrobial peptides, which lose antimicrobial activity in a saline environment.[24−26]

The secondary structure of CWR11 was elucidated by CD spectroscopy. In distilled water, the candidate peptide adopted a mixture of α-helical and β-sheet conformation, while in membrane-mimicking SDS, CWR11 assembled into a α-helical conformation (Figure 2). Secondary structure enhancement in the presence of lipid mimicking molecules is commonly observed in most naturally occurring α-helical AMPs, which has been hypothesized to be attributed to increased electrostatic interaction between the peptide and the micelle.[27−29]

In the presence of PBS, CWR11 also showed high α-helicity. It is hypothesized that electrostatic repulsion between the positive charges is reduced in the presence of salt, which could lead to increased interchain hydrophobic interaction.[30] As such, the high α-helicity observed could be attributed to the cumulative effect of helix formation due to interchain interactions.

CWR11 was further investigated for its antimicrobial action toward bacterial cells through FESEM, NPN fluorescence uptake, and PI leakage assays. FESEM analysis of the peptide-treated bacteria showed severe membrane disruption, which confirms the membrane disrupting ability of the peptide. This observation was further supported by results from the NPN uptake and PI leakage assay, where increased NPN and PI fluorescence in a dose-dependent pattern suggested the potent membrane-perturbing ability of CWR11.

The excellent antimicrobial characteristics and salt-tolerant properties of CWR11 merit further studies to evaluate the peptide's potential as an antimicrobial coating agent on biomedical devices. The short length of CWR11 is also advantageous in facilitating inexpensive and easy synthesis. Because of the high occurrence rate of nosocomial bacterial infection in various settings involving the use of biomedical devices such as stents and catheters,[31,32] there is an urgent need for the development of antimicrobial surfaces, which are both bactericidal and antibiofilm. AMP immobilization on biomedical device relevant surfaces promises to improve antimicrobial functionalization of these devices, without easily evoking antibiotic resistance in pathogens.

4.2. CWR11 Immobilization on PDMS Slides. Most biomedical implantables are made of silicone polymeric materials,[33] with PDMS being one of the most widely used materials for permanent or short-term implantation.[34] In view of this, an immobilization platform using PDMS was developed for CWR11 immobilization studies.

Current immobilization methods involve multiple reaction steps, with extensive use of a variety of chemicals. To circumvent problems associated with process complexity and specificity, we developed an immobilization platform comprising a plasma-based polymerization reaction, coupled with the use of a heterobifunctional PEG spacer (NH_2−PEG−Mal). The maleimide group attached at the end of each PEG chain allows specificity for peptide-derived cysteine attachment, and minimizes nonspecific reactions between the peptide and polymer brush.

The first step of the immobilization process utilized continuous plasma to activate the PDMS surface with radicals that are highly reactive to specific chemical groups.[35] Following surface activation, the PDMS was immersed in 100% AGE monomer solution, and exposed to UV to impart reactive epoxide groups onto the PDMS surface. This treatment yields extensive polymer brush formation on the PDMS surfaces with epoxide groups exposed at the end of each chain, which then reacted with the amine group from the bifunctional PEG moiety (NH_2−PEG−Mal). The epoxide−amine addition reaction is fairly reactive, with a reported activation energy of ~63 kJ/mol.[36] Completion of this reaction would lead to the formation of AGE polymer brushes with long PEG spacers, and maleimide groups exposed at the end of each chain (PDMS−AGE−PEG). The diffusional and conformational flexibility provided to the peptide by the relatively long PEG spacer (323 nm)[37] is expected to enhance peptide−bacterial interaction. Lastly, specific sulfhydryl coupling between maleimide groups and cysteines of CWR11 facilitated the immobilization of CWR11 to the polymer brushes.

Various assays were conducted to characterize the peptide-immobilized PDMS surface and verify the successful tethering of CWR11 onto the polymer brush. Contact angle measurement at different stages of chemical reaction on the PDMS slides demonstrated that a relatively hydrophilic surface was

formed upon peptide immobilization, which is due to the combined effect of hydrophilic AGE and peptide. The same observation was reported by Gao et al.,[38] where a final contact angle of ∼60° was attained upon peptide immobilization. Identification of distinctive amide I (1653 cm^{-1}) and II (1558 cm^{-1}) bands using ATR-FTIR further confirmed the successful immobilization of CWR11 onto the respective PDMS surfaces. This result agrees with previous studies on characterizing attachment of peptides onto activated surfaces. For example, covalent immobilization of laminin onto treated chitosan surfaces were also verified by the presence of absorption bands at 1665 cm^{-1} and 1543 cm^{-1}.[39]

Sulfo-SDTB spectrophotometric assay estimated an immobilized peptide concentration of 0.8 ± 0.2 μg of CWR11 per square centimeter of PDMS slides. This concentration agrees well with other antimicrobial peptide immobilization studies reported using different coupling strategies.[40,41] In comparison with conventional grafting methods, which require a large amount of different chemicals and complex reaction steps,[38,42] this platform provides a simpler avenue for site-specific immobilization of peptides involving only three simple reaction steps. The use of a simple heterobifunctional PEG spacer enables the direct immobilization of cysteine-terminated peptides onto AGE polymer brushes, bypassing cumbersome chemical modification steps.

The antimicrobial property of the peptide-immobilized PDMS slides was quantitatively assessed via a protocol adapted from ISO 22961.[43] Complete growth inhibition was observed for the three target bacterial strains (*E. coli*, *S. aureus*, and *P. pseudomonas*). Good peptide stability was also observed, with the peptide-immobilized slides retaining bactericidal properties for up to 3 days of immersion under soft cleaning conditions.

Biofilm formation is another important aspect of nosocomial infection that must be addressed. It is well-known that biofilms are difficult to eradicate and have rendered conventional antibiotics less effective.[44] Hence, it is essential that the peptide-immobilized surface should not only be antimicrobial but also antibiofilm. Both crystal violet staining and LIVE/DEAD staining results demonstrate that the CWR11-immobilized PDMS slide surfaces do not support bacterial cell attachment, hence preventing the formation of biofilm. The increase in surface hydrophilicity upon modification of the PDMS surface with PEG spacers and peptides is believed to contribute to the observed antibiofilm property. Such antibiofilm property makes the peptide-loaded surface a superior choice, compared to other antibiotic loading techniques, which is not only relatively ineffective in overcoming bacteria biofilm formation,[45] but has a high tendency to promote antibiotic resistance development.

Cytotoxicity is of utmost importance for biomedical implants. Conventional antimicrobial materials such as Ag ions are not widely utilized for surface coating, despite their potent bactericidal property, because of their high cytotoxicity at moderate concentration.[46] The CWR11-immobilized PDMS slides were subjected to hemolytic assay and found to be noncytotoxic, with a hemolysis rate at ∼2.0%, which is comparable to that reported by other biocompatible antimicrobial surfaces.[47,48] When the slides were challenged with smooth muscle cells, the cells grew well on the surfaces, up to 7 days, showing good cell viability (see Figures 9B and 9C). This result demonstrates that the CWR11-immobilized slides showed good selectivity toward bacteria cells and not mammalian cells, and opens the way for the use of this biomedical-device-relevant surface for antimicrobial functionalization.

5. CONCLUSIONS

We successfully engineered a novel synthetic arginine- and tryptophan-rich antimicrobial peptide (AMP), CWR11, which possessed potent bactericidal properties and salt-resistant traits. The low submolar minimum inhibitory concentration (MIC) of CWR11 against all the bacteria strains studied—and, in particular, *S. aureus*—indicates that CWR11 is highly potent, relative to conventional antibiotics, and justifies further study to evaluate the peptide's potential an antimicrobial coating for biomedical device. We subsequently developed a simple three-step covalent immobilization platform to tether CWR11 onto a silicone substrate. The immobilization strategy employs a heterobifunctional polyethylene glycol (PEG) spacer, which covalently links the peptide to the allyl glycidyl ether (AGE) polymer brush, to reduce tethering complexity and improve grafting efficiency. Surface characterization assays including X-ray photoelectron spectroscopy (XPS) and attenuated total reflectance−Fourier transform infrared spectroscopy (ATR-FTIR) confirmed the successful grafting of CWR11 onto the polymethylsiloxane (PDMS) surface. The CWR11-impregnated surface showed potent, broad spectrum antimicrobial and antibiofilm characteristics, and is noncytotoxic toward mammalian cells. These results now open the door to using CWR11 as a potential peptide candidate to protect implants from bacteria colonization.

AUTHOR INFORMATION

Corresponding Author

*Tel.: +65 6316 8775. Fax +65 6794 7553. E-mail address: SLeong@ntu.edu.sg.

Notes

The authors declare no competing financial interest.

ACKNOWLEDGMENTS

S.S.J.L. and P.A.T. would like to acknowledge the financial support from the Biomedical Engineering Program, A*Star (BEP 103149001) to perform this work. We would also like to thank Li Peng for conducting the MTT assay reported in this study.

ACRONYMS AND ABBREVIATIONS

AGE = allyl glycidyl ether
AMP = antimicrobial peptide
ATR-FTIR = attenuated total reflectance−Fourier transform infrared spectroscopy
CD = circular dichroism
EDS = energy-dispersive X-ray spectroscopy
FESEM = field-emission scanning electron microscopy
MIC = minimum inhibitory concentration
MTT = methyl tetrazolium
NPN = 1-*N*-phenylnapthylamine
PBS = phosphate buffer saline
PDMS = polymethylsiloxane
PEG = polyethylene glycol
PI = propidium iodide
SDS = sodium dodecyl sulfate
XPS = X-ray photoelectron spectroscopy

REFERENCES

(1) De Lucca, A. J.; Walsh, T. J. *Antimicrob. Agents Chemother.* **1999**, *43*, 1−11.
(2) Theis, T.; Stahl, U. *Cellular and Molecular Life Sciences CMLS* **2004**, *61*, 437−455.
(3) Andersen, J. H.; Jenssen, H.; Sandvik, K.; Gutteberg, T. J. *J. Med. Virology* **2004**, *74*, 262−271.
(4) McPhee, J. B.; Scott, M. G.; Hancock, R. E. W. *Comb. Chem. High Throughput Screening* **2005**, *8*, 257−272.
(5) Yeaman, M. R.; Yount, N. Y. *Pharmacol. Rev.* **2003**, *55*, 27−55.
(6) Chan, D. I.; Prenner, E. J.; Vogel, H. J. *Biochim. Biophys. Acta* **2006**, *1758*, 1184−1202.
(7) Li, X.; Saravanan, R.; Kwak, S. K.; Leong, S. S. J. *Chem. Eng. Sci.* **2013**, *95*, 128−137.
(8) Yau, W. M.; Wimley, W. C.; Gawrisch, K.; White, S. H. *Biochemistry* **1998**, *37*, 14713−14718.
(9) Persson, S.; Antoinette Killian, J.; Lindblom, G. r. *Biophys. J.* **1998**, *75*, 1365−1371.
(10) Killian, J. A.; Salemink, I.; de Planque, M. R. R.; Lindblom, G. r.; Koeppe, R. E.; Greathouse, D. V. *Biochemistry* **1996**, *35*, 1037−1045.
(11) Pace, C. N.; Vajdos, F.; Fee, L.; Grimsley, G.; Gray, T. *Protein Sci.* **1995**, *4*, 2411−2423.
(12) Wiegand, I.; Hilpert, K.; Hancock, R. E. W. *Nat. Protocols* **2008**, *3*, 163−175.
(13) Hancock, R. E. W.; Farmer, S. W.; Li, Z.; Poole, K. *Antimicrob. Agents Chemother.* **1991**, *35*, 1309−1314.
(14) Ivanov, I. E.; Morrison, A. E.; Cobb, J. E.; Fahey, C. A.; Camesano, T. A. *ACS Appl. Mater. Interfaces* **2012**, *4*, 5891−5897.
(15) Vreuls, C.; Zocchi, G.; Thierry, B.; Garitte, G.; Griesser, S. S.; Archambeau, C.; Van De Weerdt, C.; Martial, J.; Griesser, H. *J. Mater. Chem.* **2010**, *20*, 8092−8098.
(16) Oren, Z.; Shai, Y. *Biochemistry* **1997**, *36*, 1826−1835.
(17) Hancock, R. E. W.; Wong, P. G. W. *Antimicrob. Agents Chemother.* **1984**, *26*, 48−52.
(18) Mishra, B.; Leishangthem, G. D.; Gill, K.; Singh, A. K.; Das, S.; Singh, K.; Xess, I.; Dinda, A.; Kapil, A.; Patro, I. K.; Dey, S. *Biochim. Biophys. Acta* **2013**, *1828*, 677−686.
(19) Wong, I.; Ho, C. M. *Microfluidics Nanofluidics* **2009**, *7*, 291−306.
(20) Gaur, R. K.; Gupta, K. C. *Anal. Biochem.* **1989**, *180*, 253−258.
(21) Stepanović, S.; Vuković, D.; Dakić, I.; Savić, B.; Švabić-Vlahović, M. *J. Microbiol. Methods* **2000**, *40*, 175−179.
(22) Aliste, M. P.; MacCallum, J. L.; Tieleman, D. P. *Biochemistry* **2003**, *42*, 8976−8987.
(23) Peschel, A.; Jack, R. W.; Otto, M.; Collins, L. V.; Staubitz, P.; Nicholson, G.; Kalbacher, H.; Nieuwenhuizen, W. F.; Jung, G.; Tarkowski, A.; van Kessel, K. P. M.; van Strijp, J. A. G. *J. Exp. Med.* **2001**, *193*, 1067−1076.
(24) Goldman, M. J.; Anderson, G. M.; Stolzenberg, E. D.; Kari, U. P.; Zasloff, M.; Wilson, J. M. *Cell* **1997**, *88*, 553−560.
(25) Turner, J.; Cho, Y.; Dinh, N. N.; Waring, A. J.; Lehrer, R. I. *Antimicrob. Agents Chemother.* **1998**, *42*, 2206−2214.
(26) Park, I. Y.; Cho, J. H.; Kim, K. S.; Kim, Y. B.; Kim, M. S.; Kim, S. C. *J. Biol. Chem.* **2004**, *279*, 13896−13901.
(27) Wiradharma, N.; Khoe, U.; Hauser, C. A. E.; Seow, S. V.; Zhang, S.; Yang, Y. Y. *Biomaterials* **2011**, *32*, 2204−2212.
(28) Dathe, M.; Wieprecht, T. *Biochim. Biophys. Acta* **1999**, *1462*, 71−87.
(29) La Rocca, P.; Biggin, P. C.; Tieleman, D. P.; Sansom, M. S. P. *Biochim. Biophys. Acta* **1999**, *1462*, 185−200.
(30) Perez-Paya, E.; Houghten, R. A.; Blondelle, S. E. *Biochem. J.* **1994**, *299*, 587−591.
(31) Trautner, B. W. *Curr. Opin. Infect. Dis.* **2010**, *23*, 76−82.
(32) Richards, M. J. M. F.; Edwards, J. R. M. S.; Culver, D. H. P.; Gaynes, R. P. *Infect. Control Hosp. Epidemiol.* **2000**, *21*, 510−515.
(33) Bernik, D. L. *Recent Pat. Nanotechnol.* **2007**, *1*, 186−192.
(34) Pfleiderer, B.; Xu, P.; Ackerman, J. L.; Garrido, L. *J. Biomed. Mater. Res.* **1995**, *29*, 1129−1140.
(35) Siow, K. S.; Britcher, L.; Kumar, S.; Griesser, H. J. *Plasma Processes Polym.* **2006**, *3*, 392−418.
(36) Hirai, T.; Kawasaki, K.; Tanaka, K. *Phys. Chem. Chem. Phys.* **2012**, *14*, 13532−13534.
(37) Han, H. J.; Kannan, R. M.; Wang, S.; Mao, G.; Kusanovic, J. P.; Romero, R. *Adv. Funct. Mater.* **2010**, *20*, 409−421.
(38) Gao, G.; Lange, D.; Hilpert, K.; Kindrachuk, J.; Zou, Y.; Cheng, J. T. J.; Kazemzadeh-Narbat, M.; Yu, K.; Wang, R.; Straus, S. K.; Brooks, D. E.; Chew, B. H.; Hancock, R. E. W.; Kizhakkedathu, J. N. *Biomaterials* **2011**, *32*, 3899−3909.
(39) Matsuda, A.; Kobayashi, H.; Itoh, S.; Kataoka, K.; Tanaka, J. *Biomaterials* **2005**, *26*, 2273−2279.
(40) Gabriel, M.; Nazmi, K.; Veerman, E. C.; Nieuw Amerongen, A. V.; Zentner, A. *Bioconjugate Chem.* **2006**, *17*, 548−550.
(41) Lu, S. Immobilization of antimicrobial peptides onto titanium surfaces. Thesis, University of British Columbia, 2009.
(42) Gao, G.; Yu, K.; Kindrachuk, J.; Brooks, D. E.; Hancock, R. E. W.; Kizhakkedathu, J. N. *Biomacromolecules* **2011**, *12*, 3715−3727.
(43) Kowalczuk, D.; Ginalska, G. y.; Golus, J. *Int. J. Pharm.* **2010**, *402*, 175−183.
(44) Onaizi, S. A.; Leong, S. S. J. *Biotechnol. Adv.* **2011**, *29*, 67−74.
(45) Lawson, M. C.; Hoth, K. C.; DeForest, C. A.; Bowman, C. N.; Anseth, K. S. *Clin. Orthop. Relat. Res.* **2010**, *468*, 2081−2091.
(46) Wise, J. P., Sr; Goodale, B. C.; Wise, S. S.; Craig, G. A.; Pongan, A. F.; Walter, R. B.; Thompson, W. D.; Ng, A.-K.; Aboueissa, A.-M.; Mitani, H.; Spalding, M. J.; Mason, M. D. *Aquat. Toxicol.* **2010**, *97*, 34−41.
(47) Bagheri, M.; Beyermann, M.; Dathe, M. *Antimicrob. Agents Chemother.* **2009**, *53*, 1132−1141.
(48) Hilpert, K.; Elliott, M.; Jenssen, H.; Kindrachuk, J.; Fjell, C. D.; Körner, J.; Winkler, D. F. H.; Weaver, L. L.; Henklein, P.; Ulrich, A. S.; Chiang, S. H. Y.; Farmer, S. W.; Pante, N.; Volkmer, R.; Hancock, R. E. W. *Chem. Biol.* **2009**, *16*, 58−69.